Optimizing Light Intensity with PID Control

Eriko Alfian [1], Alfian Ma'arif [2,*], Phichitphon Chotikunnan [3], Ahmed Jaber Abougarair [4]
[1,2] Department of Electrical Engineering, Universitas Ahmad Dahlan, Yogyakarta, Indonesia
[3] College of Biomedical Engineering, Rangsit University, Pathum Thani 12000, Thailand
[4] Electrical and Electronics Engineering, University of Tripoli, Tripoli, Libya
Email: [1] ricoalvian945@gmail.com, [2] alfian.maarif@te.uad.ac.id
*Corresponding Author

Abstract— **Lighting is a fundamental cornerstone within interior design, possessing the capability to metamorphose spaces and evoke emotional responses profoundly. This principle applies to residential, industrial, and office domains, where lighting nuances are meticulously adjusted to enhance comfort and practicality. However, adequate luminance frequently intersects with energy wastage, often attributed to negligent light management practices. Mitigating this issue necessitates integrating light intensity controls adept at adapting to ambient luminosity and room-specific parameters. A prospective avenue encompasses incorporating a Proportional Integral Derivative (PID) control system synergized with light sensors. This research Implementing a closed-loop architecture, PID control utilizes feedback mechanisms to improve the precision of instrumentation systems. The PID methodology, consisting of Proportional, Integral, and Derivative control modalities, produces stable responses, accelerates system reactions, and diminishes deviations and overshooting by predetermined setpoints. The proposed Light Intensity Control System underpinned by PID methodology manifests as an exhibition of compelling outcomes drawn from empirical trials. The judicious selection of optimal parameters, specifically Kp = 0.2, Ki = 0.1, and Kd = 0.1, yielded noteworthy test outcomes: an ascent time of 0.0848, an overshoot of 6.5900, a culmination period of 0.4800, a settling period of 2.3032, and a steady-state error of 0.0300. Within this system, the PID controller assumes a pivotal role, orchestrating the regulation and meticulous calibration of light intensity to harmonize with designated criteria, thus fostering an environment of augmented energy efficiency and adaptability in illumination.**

***Keywords*—Light Intensity, PID, Control System.**

I. Introduction

The significance of light as an illuminative source is expounded upon in the text. Light sources are bifurcated into natural and artificial categories. Natural light, such as sunlight, moonlight, and stars, exhibits varying intensity throughout the day and night cycles. However, it may only uniformly illuminate for part of the 24 hours. Artificial light serves to supplement illumination, enabling human activities to persist [1].

Lighting within enclosed spaces, whether residential, industrial, or office environments, is paramount to optimizing activities within. However, the energy utilization for lighting often needs to be more proficient, resulting in lights unnecessarily being active despite sufficient ambient illumination. In response to this challenge, the deployment of a light-level control system is warranted, employing a light sensor integrated with the Proportional Integral Derivative (PID) control technique [2].

The PID control technique, a closed-loop control approach, comprises three constituent control elements: Proportional (P), Integral (I), and Derivative (D). This method engenders stability, accelerates system responsiveness, and diminishes the disparity between the desired setpoint and the actual value. The Proportional Controller (P) yields an output directly proportional to the error signal. The Integral controller (I) functions to achieve a system response devoid of steady-state error, while the Differential controller (D) emulates the differentiation operation [3].

Prior research often employed Dependent Resistors (LDR) as sensors, albeit yielding suboptimal results due to their nonlinear voltage response. The BH1750 light sensor is employed to devise a DC light intensity control system, capitalizing on the PID control methodology and the Arduino Uno microcontroller. Rigorous testing involving obstacles and external light sources scrutinizes the system's performance and reliability. This systematic evaluation paves the way for potential implementation in specialized environments, necessitating precise light intensity and optimization [4].

II. Method

In the domain of Light Intensity Management, this study delved into the calibration of light intensity through a standardized photodiode sensor, employing PID control to ascertain optimal parameter settings for achieving accurate and consistent light modulation [5]. The primary objective of this investigation is to establish a regime of steady light intensity control, a critical factor in numerous applications, thereby augmenting process efficiency and dependability. The empirical outcomes obtained from these experiments are anticipated to propel the utilization of PID control in a diverse array of lighting systems, imparting substantial advancements in light intensity regulation [6].

A. PID

Light intensity management using the Proportional-Integral-Derivative (PID) controller is crucial in various applications. The PID controller finds its ubiquitous utility as a feedback control mechanism, notably in industrial control systems. Its central function involves the continuous computation of error, which signifies the distinction between the designated setpoint and the measured process variable [7]. The paramount objective revolves around the persistent attenuation of this error magnitude over time, accomplished through the nuanced manipulation of control variables. These instrumental variables encompass various factors, ranging from control valve positioning and damper aperture

adjustment to the regulation of heating element power inputs [8]. These real-time adaptations, aimed at optimizing system performance, are meticulously determined by leveraging the Proportional Controller's equation (1), the Proportional-Integral Controller's equation (2), and the PID Controller's equation (3). The PID controller empowers precise and responsive light intensity regulation by systematically integrating control algorithms, fostering enhanced energy efficiency and operational adaptability [9].

$$u = K_p e(t) \tag{1}$$

$$u = K_p e(t) + \frac{K_p}{T_i}\int_0^t e(t)dt \tag{2}$$

$$u = K_p e(t) + \frac{K_p}{T_i}\int_0^t e(t)dt + K_p T_d \frac{de(t)}{dt} \tag{3}$$

B. System Design

This research adopts a bifurcated system configuration comprising two distinctive phases. The initial phase encompasses hardware design, while the subsequent step involves software development. The system method draws guidance from well-established theories and previous research endeavors, aiming to achieve optimum results congruent with predefined expectations [10]. Fig. 1 serves as a visual representation of the evolutionary process of light intensity control for lamps facilitated by PID regulation. This investigation introduces a versatile apparatus engineered to govern light intensity utilizing PID control, applicable both indoors and outdoors. The implementation incorporates a 12V DC lamp, a photodiode sensor, an Arduino microcontroller, and an L298 motor driver [11].

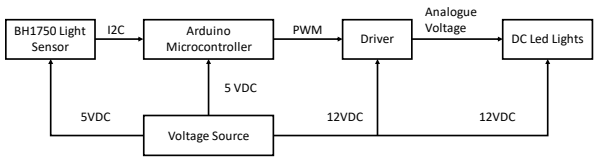

Fig. 1. Block diagram system

The block diagram of the control system is shown in Fig. 2. The reference value is adjusted to match the desired configuration, while the BH1750 sensor serves as a feedback mechanism to measure the light intensity value. The PID control computes the control signal value, determining the lamp's illumination to match the specified level [12]. The PID control system is a type of control loop feedback mechanism that uses feedback to continuously adjust the output of a process or system to match a desired setpoint. The PID controller consists of three actions: Proportional (P), Integral (I), and Derivative (D), which can produce a response with high stability and accuracy [13]. The BH1750 sensor provides 16-bit light measurements in lux, making it easy to compare against other values like references and measurements from different sensors. A PID control system with a light sensor can help regulate the light intensity in a room, adjusting it to the desired level [14].

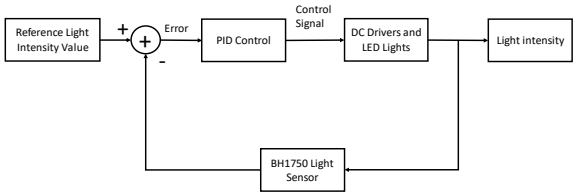

Fig. 2. Diagram block control system

C. Flowchart

Fig. 3, we present the software flowchart illustrating the operational process of a light intensity control system that utilizes PID regulation. The PID control process yields essential data outcomes and control signals. As outlined in the flowchart of Fig. 4, the initial steps involve determining the Set Point by utilizing Pulse Width Modulation (PWM) values, which are directed by photodiode sensors [15]. Subsequently, we establish the Proportional (KP), Integral (KI), and Derivative (KD) constants using a systematic trial-and-error approach. We then utilize the PWM generated by the photodiode sensors as the input for regulating DC LED lighting, effectively quantifying the emitted light intensity through digital sensors measured in lumens [16].

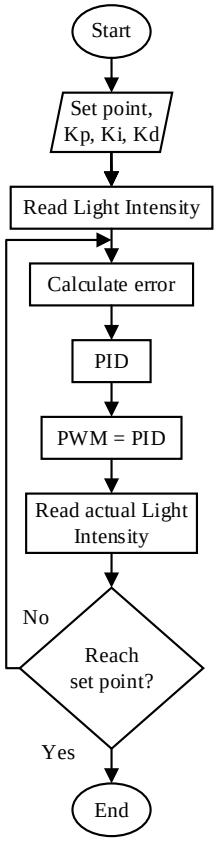

Fig. 3. Flowchart

Moving forward, we assess error values for each PID parameter by calculating the difference between the Set Point and sensor readings. This estimated error value is the input for the automated PWM adjustment, employing proportional, integral, and derivative factors. By summing the initial PWM value with the output from PID, we attain the final PWM value. The DC lamp then illuminates in response to the PWM modulation, governed by the PID controller. The sensor-

acquired measured light intensity serves as the Present Value (PV), which subsequently undergoes a comparative assessment against the Set Point [17]. This analysis achieves stability by converging the PID-regulated light intensity (PV) with the Set Point. When discrepancies arise between the Present Value (PV) and the Set Point (SP), the system performs iterative error recalculation until stability is reached. This iterative process facilitates continuous error correction, ensuring alignment with the desired outcomes [18].

D. Wiring Diagram

The hardware development phase advances through constructing the wiring diagram for the utilized components, and Fig. 4 illustrates the wiring diagram of the light intensity control system [19]. The process of creating the wiring diagram entails the establishment of connections between components using cables, thereby facilitating intercommunication among diverse elements. This wiring diagram is formulated and assembled utilizing the Fritzing application. Each component necessitates linkage to the Arduino Uno microcontroller, and additionally, connection to a power source is established via a power supply spanning from 5V to 12V [20].

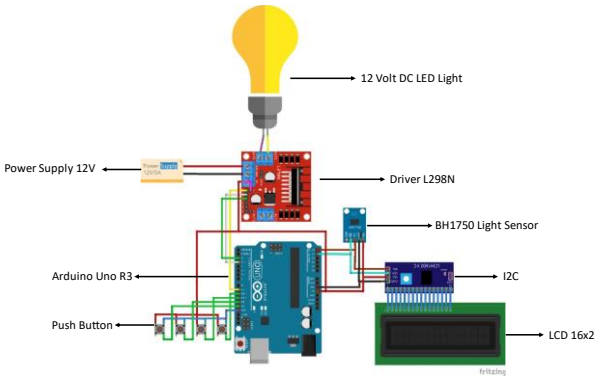

Fig. 4. Wiring diagram

III. Results and Discussion

Within Light Intensity Management, this research delves into light intensity modulation by utilizing the PID Controller. The investigation focuses on conducting an intricate evaluation of the PID methodology concerning the regulation of light intensity. This study systematically scrutinizes the dynamics of time-efficient responses and illumination outcomes by incorporating PID control. A thorough examination of PID parameters and their consequential influence on the performance of the light-intensity management system constitutes a pivotal aspect of this research endeavor.

The overarching objective is to comprehensively comprehend the efficacy and resilience of the PID Controller in effectively orchestrating precise control over light intensity. The empirical insights derived from this study are strategically poised to significantly advance the adoption of PID control techniques across a diverse spectrum of illumination systems, thereby catalyzing notable enhancements in energy efficiency, adaptability, and overall system reliability.

A. Experimental of Lux Meter and Data Actuator in PWM

Fig. 5 illustrates the procedures for testing both the sensor and actuator components. The sensor testing process directly compares the BH1750 light sensor and the LX1010B lux meter. This comparison is conducted by energizing the lamp by applying a voltage to the driver, enabling the sensor and the lux meter to measure the resulting light intensity concurrently.

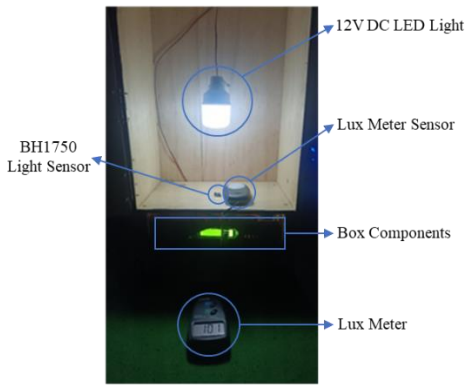

Fig. 5. Experimental sensor and actuator

Conversely, the actuator data testing focuses on the actuator's response to varying PWM voltages ranging from 25 to 250. By administering these voltage inputs to the driver, the lamp illuminates proportionally. The comprehensive outcomes of these evaluations are presented in Table 1, capturing the data gleaned from both the sensor and actuator testing methodologies.

Table 1. Experimental sensor and actuator

PWM	Analog Voltage (volt)	Light Sensor BH1750 (lux)	Lux Meter LX1010B (lux)	Error value
25	4.26	83	92	9.7%
50	5.24	165	177	6.7%
75	6.21	245	260	5.7%
100	8.01	320	342	6.4%
125	9.46	395	419	5.7%
150	9.93	465	494	5.8%
175	10.1	533	564	5.4%
200	10.43	605	640	5.4%
225	10.55	672	717	6.2%
250	10.96	744	788	5.5%
		Average		6.3%

Table 1 comprehensively presents sensor test data conducted using a lux meter and actuator test data utilizing PWM. The systematic exploration of these data sheds light on the intricate relationships between variables and system behavior. The initial driver test involved the application of a PWM voltage of 25, resulting in an analog voltage of 4.26 volts. In this scenario, the sensor detected a light intensity of 83 lux, while the lux meter recorded 92 lux, yielding an error value of 9.7%. This error represents the discrepancy between the sensor's reading and the lux meter's measurement, showcasing the precision of measurement instruments.

Continuing the investigation, we conducted additional tests involving two to ten drivers, assigning incremental PWM voltages to each. These tests consistently revealed a proportional response between PWM voltage increments and analog voltage values and subsequently detected light

intensities. An intriguing observation was the direct correspondence between increasing PWM voltage and amplifying analog voltage, a relationship fundamental to the system's response mechanism. Correspondingly, the luminous intensity of the lamp displayed a heightened radiance in line with elevated PWM voltages, highlighting the dynamic interplay between voltage inputs and light outputs.

Furthermore, the correlation between sensor-detected lux values and the associated lux meter measurements demonstrated a trend towards elevated values with increasing PWM voltages. This alignment further underscores the harmonious interrelationship between these two measurement methods. Notably, the smallest sensor-detected value was 83 lux at PWM 25, while the highest was 744 lux at PWM 250. Similarly, the minor lux meter reading was 92 lux at PWM 25, whereas the most extensive reading reached 788 lux at PWM 250. Error values ranged from 5.4% as the smallest to 9.7% as the largest, with an average error value of 6.3%. These insights contribute to a deeper understanding of the system's behavior and hold implications for fine-tuning and optimizing light intensity control mechanisms.

B. Sensor Calibration with Regression Linear

We conducted calibration testing by comparing the BH1750 light sensor and the LX1010B lux meter, aligning and calibrating the sensor-detected values with the measuring instrument. The voltage was supplied to the driver during this procedure, initiating the lamp's illumination. Simultaneously, the sensor and the lux meter detected the light intensity emanating from the lamp in parallel.

Using linear regression for the calibration process reduced the discrepancies between the values detected by the sensor and the measurements recorded by the lux meter. This achievement resulted in a noteworthy improvement in the system's precision and stability. The range of PWM voltages spanned from 25 to 250. The comprehensive dataset stemming from the sensor calibration testing, utilizing the linear regression approach, is systematically outlined in Table 2.

Table 2. Sensor Calibration

PWM	Light Sensor BH1750 (lux)	Lux Meter LX1010B (lux)	Error value
25	90	88	2.2%
50	167	164	1.8%
75	237	230	3.0%
100	327	323	1.2%
125	409	407	0.4%
150	479	478	0.2%
175	548	545	0.5%
200	619	615	0.6%
225	688	685	0.4%
250	758	755	0.3%
Average			1.1%

Table 2 comprehensively presents the outcomes of the calibration test data utilizing the linear regression approach. The initial examination involved subjecting the driver to a PWM voltage of 25, resulting in a sensor-detected value of 90 lux, a lux meter-detected value of 88 lux, and an error value of 2.2%. Notably, this initial test exhibited a narrower discrepancy in error values compared to the earlier sensor tests. Applying the linear regression method contributed to mitigating variations between the values ascertained by the lux meter measuring instrument and those by the sensor.

Subsequent examinations extended to two through ten drivers, with incremental PWM voltages applied. For instance, when testing two drivers with a PWM voltage of 50, the sensor detected a value of 167 lux, while the lux meter detected 164 lux, resulting in an error value of 1.8%. Similarly, testing three drivers with a PWM voltage of 75 yielded a sensor-detected value of 237 lux and a lux meter-detected value of 230 lux, leading to an error value of 3%. Comparable patterns persisted across the remaining tests, involving four to ten drivers, each assessed at varying PWM voltages. The calibration process with the linear regression method consistently exhibited a trend of reducing the error values, enhancing the alignment between sensor and lux meter readings, thus fostering a more accurate and stable system.

The data analysis unveiled that the lux values detected by the sensor and lux meter increased proportionally with higher PWM voltage values. Similarly, the lamp's luminosity intensified with the escalation of applied PWM voltages. Among the recorded values, the minimum sensor-detected value was 90 lux at PWM 25, while the maximum was 758 lux at PWM 250. Likewise, the smallest lux meter-detected value was 88 lux at PWM 25, and the highest was 755 lux at PWM 250. Regarding error, the range extended from 0.2% as the smallest to 2.2% as the largest. The average cumulative mistake resulting from the linear regression calibration testing amounted to 1.1%.

C. Proportional Controller

The evaluation of the proportional control system entails a systematic exploration involving the variation of Kp values, with Ki and Kd parameters fixed at 0. This experimentation aims to implement the light intensity control system by integrating PID control. The comprehensive range of Kp values (Kp = 0.1, Kp = 0.2, Kp = 0.3, Kp = 0.4, Kp = 0.5) is the variation value, enabling extensive scrutiny of the system's responses. These responses are adeptly portrayed using the PID-controlled light intensity control tool and depicted graphically in Fig. 6. Through the discerning analysis of these outcomes, a nuanced understanding is gained regarding the influence of diverse Kp values on the control system's behavior, thereby illuminating its capacity to achieve desired light intensity levels.

Table 3 presents the outcomes of the proportional control system testing, wherein a series of tests were conducted with varying proportional gain (Kp) values while keeping integral (Ki) and derivative (Kd) values at 0. In the first test, Kp was set to 0.1, resulting in undefined parameters rise time (NaN) and settling time (NaN), exhibiting a peak time of 0.4800 seconds and a significant steady-state error of 148.8000. The subsequent test was executed with Kp as 0.2, yielding analogous results with NaN rise and settling times, a peak time of 0.4800 seconds, and a reduced steady-state error of 119.7500. The third test involved Kp set at 0.3, yielding consistent NaN rise and settling times, a 0.4800-second peak time, and further reduction in steady state error to 95.9800.

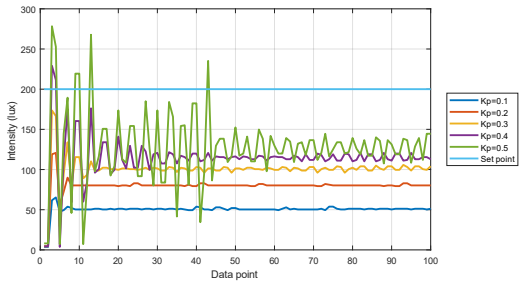

Fig. 6. Proportional controller response system

Table 3. Response system Proportional Controller

Kp	Rise Time (TR)	Overshoot (MP)	Peak Time (TS)	Settling Time (TS)	Steady State Error
0.1	NaN	0	0.4800	NaN	148.8000
0.2	NaN	0	0.4800	NaN	119.7500
0.3	NaN	0	0.4800	NaN	95.9800
0.4	0.0836	14.5100	0.3600	NaN	87.1800
0.5	0.0682	39.1600	0.3600	NaN	55.4900

For the fourth test, Kp was raised to 0.4, leading to improved parameters, including a rise time of 0.0836 seconds, overshoot of 14.5100, peak time of 0.3600 seconds, undefined settling time (NaN), and a steady state error of 87.1800. In the fifth test, Kp was increased to 0.5, resulting in enhanced system dynamics reflected by a rise time of 0.0682 seconds, considerable overshoot of 39.1600, a peak time of 0.3600 seconds, undefined settling time (NaN), and a further reduced steady-state error of 55.4900. Notably, the variations in Kp values influence system response, notably impacting oscillation amplitude, rise time reduction, slight alterations in settling time, increased overshoot, and diminished steady-state error.

D. Proportional Integral Controller

Examining the proportional-integral control system entails systematically incorporating distinct Kp and Ki values into the light intensity control system's programming, employing PID control methodology. The selection of a Kp value of 0.3, derived from optimal outcomes in the proportional control system test, is coupled with a range of Ki values, specifically Ki = 0.01, Ki = 0.02, Ki = 0.03, Ki = 0.04, and Ki = 0.05. The Kd value remains fixed at 0, underscoring the exclusive focus on the proportional and integral control elements. Proportional integral controller system shown in Fig. 7.

The varied Ki values are judiciously employed to observe the ensuing system responses, captured graphically via the PID-controlled light intensity control system tool. This graphical representation elucidates the impact of integrating an integral control system into the system response graph. The outcomes of this comprehensive analysis are effectively depicted in Fig. 8, which illustrates the results of the light intensity test across the proportional-integral control. Additionally, Table 4 briefly outlines the proportional-integral control system test findings.

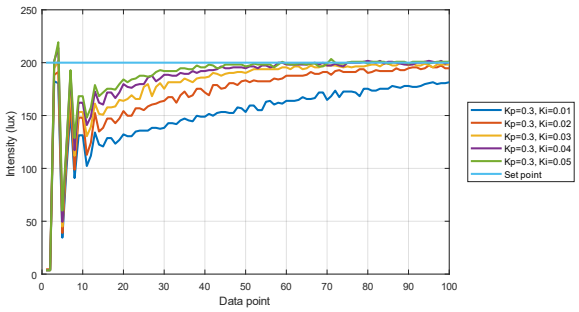

Fig. 7. Proportional integral controller system

Table 4. Response system proportional integral controller

Kp	Ki	Rise Time (TR)	Overshoot (MP)	Peak Time (TS)	Settling Time (TS)	Steady State Error
0.3	0.01	0.1055	0	0.3600	NaN	18.5100
0.3	0.02	0.1020	0	11.4000	NaN	5.3100
0.3	0.03	0.0987	0.8650	0.4800	NaN	1.7900
0.3	0.04	0.0952	0	0.4800	6.7886	0.8500
0.3	0.05	0.0956	9.6700	0.4800	6.8629	0.8500

Table 4 presents the outcomes of the proportional-integral control system assessment. The initial trial encompassed a Kp value of 0.3, with a Ki value of 0.01 and a Kd value of 0. The obtained results from this trial exhibited a rise time of 0.1055 seconds, no overshoot, a peak time of 0.3600 seconds, undefined settling time (NaN), and a steady state error of 18.5100. NaN, denoting "Not a Number," designates an undefined numerical value often encountered in floating-point arithmetic. In the subsequent trial, using the same Kp of 0.3, the Ki value was adjusted to 0.02, yielding parameters of 0.1020 seconds for rise time, no overshoot, an extended peak time of 11.4000 seconds, undefined settling time (NaN), and a steady state error of 5.3100.

Similarly, with Kp set at 0.3, the third test incorporated a Ki value of 0.03, yielding a rise time of 0.0987 seconds, 0.8650 overshoot, a peak time of 0.4800 seconds, undefined settling time (NaN), and a steady state error of 1.7900. The subsequent trial involved Kp at 0.3, Ki at 0.04, and Kd at 0, resulting in a rise time of 0.0952 seconds, no overshoot, a peak time of 0.4800 seconds, settling time of 6.7886 seconds, and a steady state error of 0.8500. The fifth trial, maintaining Kp at 0.3, incorporated a Ki value of 0.05 and Kd of 0, revealing a rise time of 0.0956 seconds, an overshoot of 9.6700, a peak time of 0.4800 seconds, a settling time of 6.8629 seconds, and a steady state error of 0.8500. Notably, the variation in Ki values significantly influences system response dynamics, affecting rise time reduction, augmented settling time, increased overshoot, and diminished steady-state error.

E. Proportional Integral Derivative (PID) Controller

The assessment of the proportional-integral-derivative (PID) control system is meticulously conducted by inputting Kp, Ki, and Kd values into the light intensity control system's software and hardware infrastructure, leveraging PID control methodology. Within this framework, a Kp value of 0.3, derived from the optimal proportional control system test results, is assigned. Similarly, the Ki value is set to 0.04, chosen based on the superior outcomes. For the Kd parameter, a spectrum of values is employed: Kd = 0.01, Kd = 0.02, Kd = 0.03, Kd = 0.04, and Kd = 0.05. The deliberate

variation of the Kd values is undertaken to observe the resultant system responses, visualized in graphical format using the light intensity control system integrated with PID control. This graphical representation offers insights into the impact of incorporating derivative control on the system response graph. The culmination of this rigorous analysis is visually presented in Fig. 9, which effectively illustrates the outcomes of the light intensity testing conducted using the PID controller, showcasing the diverse tested parameter values. Furthermore, Table 5 concisely presents the findings derived from the comprehensive evaluation of the proportional-integral-derivative control system.

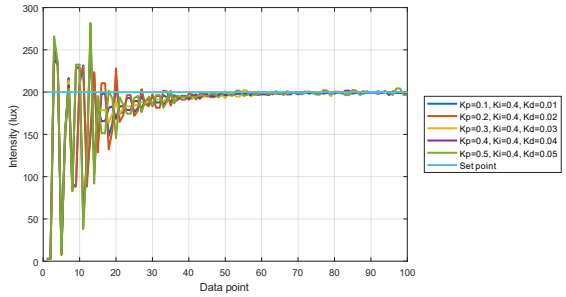

Fig. 8. PID controller system

Table 5. Response system PID controller

Kp	Ki	Kd	Rise Time (TR)	Overshoot (MP)	Peak Time (TS)	Settling Time (TS)	Steady State Error
0.3	0.04	0.01	0.0800	0	0.3600	5.3462	0.0300
0.3	0.04	0.02	0.0774	23.7550	0.3600	9.4910	1.7900
0.3	0.04	0.03	0.0752	34.7600	1.5600	9.4932	0.9100
0.3	0.04	0.04	0.0739	35.6400	1.5600	5.7331	2.6700
0.3	0.04	0.05	0.0719	40.9200	1.5600	11.7664	3.5500

Table 5 presents the report of the proportional-integral-derivative (PID) control system test. The Kp parameter value is adopted from the P control test, the Ki parameter value is derived from the I control test, and a range of Kd parameter values is considered: Kd = 0.01, Kd = 0.02, Kd = 0.03, Kd = 0.04, and Kd = 0.05. The initial test is executed with Kp = 0.3, Ki = 0.04, and Kd = 0.01. The corresponding results reveal a rise time of 0.0800 seconds, zero overshoot, peak time of 0.3600 seconds, settling time of 0.3600 seconds, and a steady state error of 5.3462. In the subsequent test, Kp = 0.3, Ki = 0.04, and Kd = 0.02. The outcomes reflect a rise time of 0.0774 seconds, an overshoot of 23.7550, a peak time of 0.3600 seconds, a settling time of 9.4910 seconds, and a steady state error of 1.7900. Similarly, with Kp = 0.3, Ki = 0.04, and Kd = 0.03, the results encompass a rise time of 0.0752 seconds, an overshoot of 34.7600, a peak time of 1.5600 seconds, settling time of 9.4932 seconds, and a steady state error of 0.9100. The fourth scenario involves Kp = 0.3, Ki = 0.04, and Kd = 0.04, resulting in a rise time of 0.0739 seconds, an overshoot of 35.6400, a peak time of 1.5600 seconds, a settling time of 5.7331 seconds, and a steady state error of 2.6700. Lastly, with Kp = 0.3, Ki = 0.04, and Kd = 0.05, the fifth test yields a rise time of 0.0719 seconds, an overshoot of 40.9200, a peak time of 1.5600 seconds, a settling time of 11.7664 seconds, and a steady state error of 3.5500. Notably, the Kd value significantly influences the resulting system response, notably in the subtle alteration of rise time and reduction of overshoot and settling time, while having no substantial impact on steady-state error results.

F. Best Parameter PID Controller

The evaluation of the Proportional-Integral-Derivative (PID) control system entails the precise configuration of Kp, Ki, and Kd values within the light intensity control system software and hardware, employing the principles of PID control. Implementing PID control, the Light Intensity Control System reaps the benefits of meticulous data trials, with optimal outcomes derived from the selection of Kp = 0.2, Ki = 0.1, and Kd = 0.1. The system's set point is 200, with a PWM setting 25 and an Arduino program delay of 50. In this paradigm, the PID controller seamlessly functions to regulate light intensity, ensuring that stability is achieved as the light intensity approaches the predetermined set point, aligning the light intensity precisely with the designated set point. Fig. 10. shows the best PID parameter for light intensity at 200 lux. The culmination of this rigorous analysis is succinctly encapsulated in Table 6, which presents the paramount data test outcomes derived from applying the Proportional-Integral-Derivative (PID) control system to regulate light intensity.

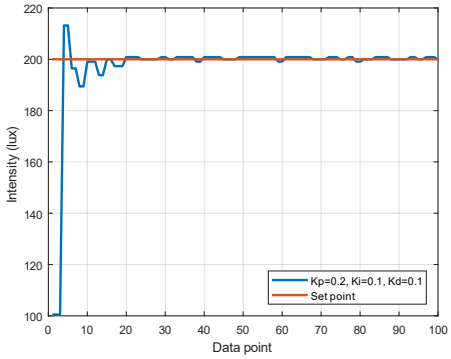

Fig. 9. The best PID parameter

Table 6. Response system the best PID controller

Kp	Ki	Kd	Rise Time (TR)	Overshoot (MP)	Peak Time (TS)	Settling Time (TS)	Steady State Error
0.2	0.1	0.1	0.0848	6.5900	0.4800	2.3032	0.0300

Table 6 shows the best data test results from the proportional-integral-derivative control system. The value of the Kp parameter uses the value from the P control test, the Ki parameter value uses the value from the control test I, and the Kd parameter value uses the value from the D control test. The test is carried out by giving a Kp value = 0.2, a Ki value = 0.1, and a value Kd = 0.1. The test results were obtained at rise time = 0.0848, overshoot = 6.5900, peak time = 0.4800, settling time = 2.3032, and steady-state error = 0.0300. Kp, Ki, and Kd values affect system response, making the resulting PID more stable.

G. Sensor Distance Experiments

The experimentation involving distance measurement through the utilization of the Proportional-Integral-Derivative (PID) control system is characterized by a meticulous selection of PID parameters, specifically Kp = 0.2, Ki = 0.1, and Kd = 0.1. The range of distances under scrutiny encompasses 0 cm, 5 cm, 10 cm, 15 cm, and 20 cm. Within this controlled environment, the Light Intensity Control System harmonizes with the principles of PID

control, orchestrating a symphony of precise data trials. The system's set point, firmly established at 200 lux.

The PID controller assumes a central role in this framework, orchestrating the symphony of light intensity regulation. Its primary objective is to ensure that the light intensity converges seamlessly towards the predefined set point of 200 lux, maintaining an impeccable alignment with the desired illumination. As a testament to the efficacy of this meticulously tailored PID setup, Fig. 10 shows the light intensity with various distance. These remarkable insights and outcomes coalesce succinctly within Table 7, an invaluable of data test results, underscoring the potency of the Proportional-Integral-Derivative (PID) control system in orchestrating precise light intensity regulation.

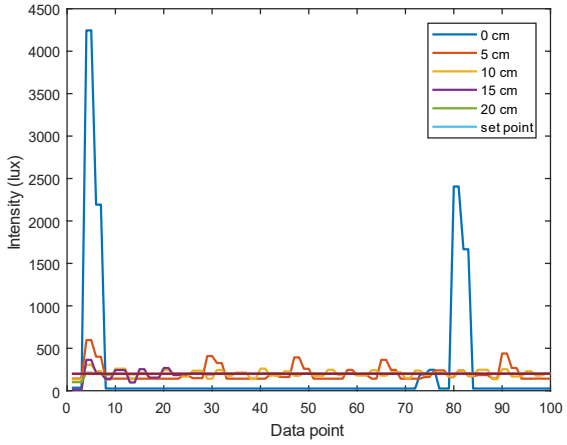

Fig. 10. Distance experimental using best PID

Table 7. Distance experimental using best PID

Distance	Rise Time	Peak Time	Settling Time	Overshoot (%)	Steady State Error
0 cm	0.03129	4	25.6700	2022.550	174.33
5 cm	0.10083	4	NaN	198.500	58.13
10 cm	0.31192	4	98.9062	52.365	0.03
15 cm	0.42714	4	87.1543	81.855	-0.85
20 cm	0.70643	4	19.1932	6.5900	0.03

Table 7 presents a comprehensive analysis of the performance of a light-intensity control system at different distances using the Proportional-Integral-Derivative (PID) control method. The distances represent the proximity of the light source to the sensor: 0 cm, 5 cm, 10 cm, 15 cm, and 20 cm. The table provides various parameters that describe the system's response characteristics.

For the case where the light source is at a distance of 0 cm, the system exhibits a very low-rise time of 0.03129 seconds, indicating a rapid response. However, the overshoot value is notably high at 2022.55%, which signifies a significant deviation from the desired light intensity. The steady-state error is also relatively high at 174.33, implying that the system does not precisely reach the desired setpoint.

When the light source is positioned 5 cm away, the rise time remains low at 0.10083 seconds, and the overshoot is reduced to 198.5%. However, the settling time is unavailable (NaN), indicating that the system is not stable within the observed time frame. The steady-state error is 58.13, indicating a significant difference between the desired and actual light intensity.

At a distance of 10 cm, the rise time is slightly higher at 0.31192 seconds. The overshoot is significantly reduced to 52.365%, suggesting a more controlled response. The settling time is 98.90619718 seconds, indicating that the system takes longer to reach a stable state. The steady-state error is minimized to 0.03, indicating a closer alignment with the desired light intensity.

Similarly, for distances of 15 cm and 20 cm, the rise times are 0.42714 seconds and 0.70643 seconds, respectively. The overshoot values decreased to 81.855% and 6.59%, indicating more controlled responses. The settling times are 87.15436364 seconds and 19.19318182 seconds, respectively. The steady-state errors are -0.85 and 0.03 for 15 cm and 20 cm, respectively. The negative steady-state error at 15 cm suggests an overcompensation, while the close-to-zero steady-state error at 20 cm signifies a good alignment with the setpoint.

In summary, the analysis of Table 7 reveals that as the distance between the light source and the sensor increases, the system response becomes more stable with reduced overshoot and steady-state error. The best performance is observed at a distance of 20 cm, where the system achieves a balanced trade-off between response speed and accuracy.

IV. CONCLUSION

Based on the conducted tests, it is evident that applying PID control to light intensity management is substantiated through a meticulously designed operational framework involving actuators, sensors, controller devices, and motor drivers. The experimental setup employs a 12 Volt DC LED lamp as the actuator, coupled with the BH1750 light sensor, Arduino UNO controller device, and the L298N motor driver. The resulting Light Intensity Control System utilizing PID control demonstrates superior performance with optimized parameters (Kp = 0.2, Ki = 0.1, Kd = 0.1), yielding precise outcomes including rise time (0.0848), overshoot (6.5900), peak time (0.4800), settling time (2.3032), and steady-state error (0.0300). The PID controller effectively regulates light intensity to desired levels, showcasing operational efficiency and rapid responsiveness. In contrast, the magnitude of light output is directly correlated to Pulse Width Modulation (PWM) levels, providing increased luminosity with higher PWM values.

REFERENCES

[1] J. S. Willems, J. N. Phillips, and C. D. Francis, "Artificial light at night and anthropogenic noise alter the foraging activity and structure of vertebrate communities," *Science of The Total Environment*, vol. 805, p. 150223, 2022, https://doi.org/10.1016/j.scitotenv.2021.150223.

[2] C. E. Reilly *et al.*, "Minimizing ecological impacts of marine energy lighting," *Journal of Marine Science and Engineering*, vol. 10, no. 3, p. 354, 2022, https://doi.org/10.3390/jmse10030354.

[3] T. George and V. Ganesan, "Optimal tuning of PID controller in time delay system: A review on various optimization techniques," *Chemical Product and Process Modeling*, vol. 17, no. 1, pp. 1–28, 2020, https://doi.org/10.1515/cppm-2020-2001.

[4] A. Mellit, M. Benghanem, O. Herrak, and A. Messalaoui, "Design of a novel remote monitoring system for smart greenhouses using the internet of things and deep convolutional Neural Networks," *Energies*, vol. 14, no. 16, p. 5045, 2021, https://doi.org/10.3390/en14165045.

[5] J. Gutiérrez Mena, S. Kumar, and M. Khammash, "Dynamic cybergenetic control of bacterial co-culture composition via optogenetic feedback," *Nature Communications*, vol. 13, no. 1, 2022, https://doi.org/10.1038/s41467-022-32392-z.

[6] V. Moudgil, K. Hewage, S. A. Hussain, and R. Sadiq, "Integration of IOT in Building Energy Infrastructure: A Critical Review on challenges and solutions," *Renewable and Sustainable Energy Reviews*, vol. 174, p. 113121, 2023, https://doi.org/10.1016/j.rser.2022.113121.

[7] J. Huang *et al.*, "AIChE PD2M advanced process control workshop-moving APC forward in the pharmaceutical industry," *Journal of Advanced Manufacturing and Processing*, vol. 3, no. 1, p. e10071, 2021, https://doi.org/10.1002/amp2.10071.

[8] S. Adomako *et al.*, "R&D intensity, knowledge creation process and new product performance: The mediating role of international r&d teams," *Journal of Business Research*, vol. 128, pp. 719–727, 2021, https://doi.org/10.1016/j.jbusres.2019.08.036.

[9] M. Ranjan and R. Shankar, "A literature survey on load frequency control considering renewable energy integration in power system: Recent trends and future prospects," *Journal of Energy Storage*, vol. 45, p. 103717, 2022, https://doi.org/10.1016/j.est.2021.103717.

[10] E. Osman, G. Hardaker, and L. E. Glenn, "Implementing structural equation modelling and multiple mediator models for Management Information Systems," *The International Journal of Information and Learning Technology*, vol. 39, no. 5, pp. 496–510, 2022, https://doi.org/10.1108/IJILT-09-2022-0182.

[11] T. T. Tharshini, E. Jeevitha, S. R. Subhiksha, H. J. Dharshini and P. S. Manoharan, "Indigenous Robot for Advanced Driver Assistance System," *2022 International Conference on Automation, Computing and Renewable Systems (ICACRS)*, pp. 1437-1440, 2022, https://doi.org/10.1109/ICACRS55517.2022.10029160.

[12] J. Niu, B. Liang, S. He, J. Xiao, and C. Qin, "Long Tunnel Lighting Environment Improvement Method based on multiple-parameter intelligent control: Considering dynamic changes in luminance difference," *Tunnelling and Underground Space Technology*, vol. 128, p. 104637, 2022, https://doi.org/10.1016/j.tust.2022.104637.

[13] F. S. M. Alkhafaji, W. Z. Wan Hasan, M. Isa, and N. Sulaiman, "A Novel Method for Tuning PID Controller", *JTEC*, vol. 10, no. 1-12, pp. 33–38, 2018, https://jtec.utem.edu.my/jtec/article/view/3821.

[14] M. S. Munir, I. S. Bajwa, M. A. Naeem, and B. Ramzan, "Design and implementation of an IOT system for smart energy consumption and smart irrigation in tunnel farming," *Energies*, vol. 11, no. 12, p. 3427, 2018, https://doi.org/10.3390/en11123427.

[15] M. K. Ghodki, A. Swarup, and Y. Pal, "A new IR and sprinkler based embedded controller directed robotic arm for automatic cleaning of solar panel," *Journal of Engineering, Design and Technology*, vol. 18, no. 4, pp. 905–921, 2019, https://doi.org/10.1108/JEDT-10-2019-0253.

[16] F. Loose, L. Teixeira, R. R. Duarte, M. A. Dalla Costa, and C. H. Barriquello, "On the use of the intrinsic ripple of a buck converter for visible light communication in LED drivers," *IEEE Journal of Emerging and Selected Topics in Power Electronics*, vol. 6, no. 3, pp. 1235–1245, 2018, https://doi.org/10.1109/JESTPE.2018.2843280.

[17] S. Gunjate And S. A. Khot, "A Systematic Review of Emergency Braking Assistant System to Avoid Accidents Using Pulse Width Modulation and Fuzzy Logic Control Integrated with Antilock Braking", *Int. J. Automot. Mech. Eng.*, vol. 20, no. 2, pp. 10457–10479, 2023, https://jtec.utem.edu.my/jtec/article/view/3821.

[18] E. Nyberg, D. Llopart i Cervelló, and I. Minami, "Tribology in space robotic actuators: Experimental method for evaluation and analysis of gearboxes," *Aerospace*, vol. 8, no. 3, p. 75, 2021, https://doi.org/10.3390/aerospace8030075.

[19] R. Wrobel and B. Mecrow, "A comprehensive review of additive manufacturing in construction of Electrical Machines," *IEEE Transactions on Energy Conversion*, vol. 35, no. 2, pp. 1054–1064, 2020, https://doi.org/10.1109/TEC.2020.2964942.

[20] A. Hameed and Y. Al-Daraje, "Establishing a Low and Variable Voltage Power Supply System with Digital Control," *2019 16th International Multi-Conference on Systems, Signals & Devices (SSD)*, pp. 242-245, 2019, https://doi.org/10.1109/SSD.2019.8893201.